# Three-Dimensional Finite-Element Analyses for Radio-Frequency Hepatic Tumor Ablation

Supan Tungjitkusolmun, *Member, IEEE*, S. Tyler Staelin, Dieter Haemmerich, *Student Member, IEEE*, Jang-Zern Tsai, *Student Member, IEEE*, Hong Cao, *Student Member, IEEE*, John G. Webster*, *Life Fellow, IEEE*, Fred T. Lee, Jr., David M. Mahvi, and Vicken R. Vorperian

***Abstract*—Radio-frequency (RF) hepatic ablation, offers an alternative method for the treatment of hepatic malignancies. We employed finite-element method (FEM) analysis to determine tissue temperature distribution during RF hepatic ablation. We constructed three-dimensional (3-D) thermal-electrical FEM models consisting of a four-tine RF probe, hepatic tissue, and a large blood vessel (10-mm diameter) located at different locations. We simulated our FEM analyses under temperature-controlled (90 °C) 8-min ablation. We also present a preliminary result from a simplified two-dimensional (2-D) FEM model that includes a bifurcated blood vessel. Lesion shapes created by the four-tine RF probe were mushroom-like, and were limited by the blood vessel. When the distance of the blood vessel was 5 mm from the nearest distal electrode 1) in the 3-D model, the maximum tissue temperature (hot spot) appeared next to electrods A. The location of the hot spot was adjacent to another electrode 2) on the opposite side when the blood vessel was 1 mm from electrode A. The temperature distribution in the 2-D model was highly nonuniform due to the presence of the bifurcated blood vessel. Underdosed areas might be present next to the blood vessel from which the tumor can regenerate.**

***Index Terms*—Bioheat equation, finite-element analysis, hepatic ablation, radio-frequency ablation.**

## I. Introduction

THE LIVER is a common location for both primary and metastatic malignancies. Annually, over one-million new patients develop hepatocellular carcinoma around the world [1]. Surgical resection is presently the treatment of choice for both well-localized primary and metastatic hepatic malignancies [2]. However, the majority of the patients are not candidates for surgical resection due to certain criteria, such as multifocal disease, tumor size, location of tumor to key vessel, or coagulopathies. Thus, there is a demand for novel minimally invasive techniques for cure of hepatic malignancies.

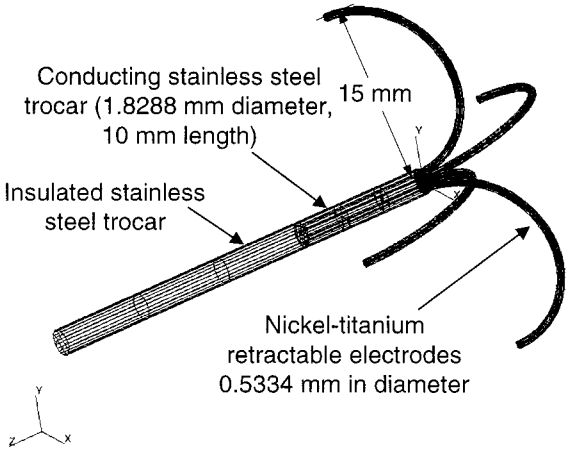


Fig. 1. The structure of the fully deployed four-tine RF probe for hepatic tumor ablation. The surface area of the last 10 mm of the trocar and the tines all conduct RF current. The orientation of the coordinates for the FEM models is also shown.

Focal ablative therapies have been developed and applied to the treatment of hepatic malignancies. Unlike surgical resection, ablative therapies are not associated with the loss of entire segments or lobes of normal liver. The most widely investigated focal ablative techniques are cryoablation and radio-frequency (RF) ablation. Although the posttreatment recurrence rate of cryoablation has been lower than RF, an open surgery is generally necessary due to large probe sizes, and the risk of bleeding. In contrast, the RF ablation procedure is safe and can be applied percutaneously since the needle probes (14–17 gauge) for RF ablation are smaller [21].

RF ablation utilizes ac current, typically at about 500 kHz, to destroy unwanted tissues by heating. Denaturation of intracellular proteins and destruction of cell membranes occur when the cells are heated to above 45 °C–50 °C [19], [20]. RF ablation has gained wide acceptance as a standard treatment for supraventricular tachycardias where the target sites are small and well defined. Successful ablation of hepatic tumor with RF energy requires accurate localization and adequate tissue destruction. Performing RF ablation aided with percutaneous image-guided techniques [computed tomography (CT), ultrasound, or magnetic resonance imaging] has a potential to be a treatment of choice for hepatic malignancies because it is minimally invasive compared with surgical resection. Although RF ablation avoids the necessity for open laparotomy, it has been associated

Manuscript received September 9, 2000; revised August 15, 2001. This work was supported by the National Institutes of Health (NIH) under Grant HL56143 and Grant DK58839. *Asterisk indicates corresponding author.*

S. Tungjitkusolmun is with the Department of Electronics Engineering, King Mongkut's Institute of Technology Ladkrabang, Ladkrabang, Bangkok 10520, Thailand

S. T. Staelin and D. M. Mahvi are with the Department of Surgery, University of Wisconsin, Madison WI 53792 USA.

D. Haemmerich is with the Department of Biomedical Engineering, University of Wisconsin, Madison, WI 53706 USA.

J.-Z. Tsai and H. Cao are with the Department of Electrical and Computer Engineering, University of Wisconsin, Madison, WI 53706 USA.

*J. G. Webster is with the Department of Biomedical Engineering, University of Wisconsin, 1415 Engineering Dr., Madison, WI 53792 USA (e-mail: webster@engr.wisc.edu).

V. R. Vorperian is with the Department of Electrophysiology, University of Wisconsin, Madison WI 53792 USA.

F. T. Lee, Jr. is with the Department of Radiology, University of Wisconsin, 1415 Engineering Dr., Madison, WI 53792 USA.

Publisher Item Identifier S 0018-9294(02)00200-8.

TABLE I
THERMAL AND ELECTRICAL PROPERTIES OF THE MATERIALS IN THE FEM MODELS

| FEM region | Material | $\rho$ [kg/m$^3$] | $c$ [J/kg·K] | $k$ [W/m·K] | $\sigma$ [S/m] |
|---|---|---|---|---|---|
| Electrode | Ni–Ti | 6450 | 840 | 18 | $1 \times 10^8$ |
| Trocar | Stainless steel | 21500 | 132 | 71 | $4 \times 10^6$ |
| Tissue | Liver | 1060 | 3600 | 0.512 | 0.333 |
| Blood | Blood | 1000 | 4180 | 0.543 | 0.667 |
| Catheter body | Polyurethane | 70 | 1045 | 0.026 | $10^{-5}$ |

with much higher local recurrence rates than hepatic resection [3]–[8].

Current RF probe designs are simple, using probe tip temperature, impedance, or power output as control parameters. The response of hepatic tissues to thermal heating depends upon several factors such as hepatic material properties, ablation duration, mode of ablation (temperature- or power-controlled), tumor location, and the geometry of the ablation probe. Since RF hepatic ablative technique is relatively new, the high local recurrence rates might be due to inadequate probe designs, placements, or overheating of the tissue in close proximity to the RF probe. These factors may contribute to incomplete destruction of tumor cells.

Mathematical modeling is a powerful tool for predicting lesion dimensions created by various RF probe designs. In order to know the change in potential and temperature distributions in the hepatic tissue during ablation, we solved the bioheat equation. As the geometries of the objects involved in RF hepatic ablation (RF probe, blood vessels, hepatic tissue) are complicated, we use FEM method models to solve the bioheat three-dimensional (3-D) FEM modeling studies of RF cardiac ablation have been presented [9]–[11]. However, no previous studies have introduced any 3-D numerical model that includes a realistic probe for hepatic RF ablation.

In this study, we modeled a commonly used (15 gauge) hepatic ablation probe [RITA Medical Systems Model 30 (RITA Medical Systems, Inc., Mountain View, CA)], situated in the middle of the hepatic tissue. We performed FEM analyses under the temperature-controlled mode (90 °C), for a duration of 8 min. We selected the temperature-controlled mode since it is more widely used in clinical practice to help reduce the incidence of overheating of the catheter–tissue interface and coagulation. We investigated the effect of the presence of a blood vessel and its distance to the electrode. We also present some preliminary results from a two-dimensional (2-D) model with a bifurcated blood vessel.

## II. METHODOLOGY

There has been little numerical study of hepatic ablation. Curley *et al.* [12] simulated a one-dimensional finite difference model for hepatic ablation. We established realistic FEM models of RF ablation probes to better understand how current flows from them to surrounding liver tissue. Fig. 1 shows the configuration of the initial probe that we modeled, a RITA Medical Systems Model 30, which is the most commonly utilized clinical system. The straight RF probe is placed into the liver tumor percutaneously under CT or ultrasound guidance. Once in place, surgeons deploy the four tines in an umbrella-like array and initiate RF current. We utilized both 3-D and simplified 2-D FEM models in this study. We also used 2-D FEM models because of the limitation of our current computing resource. Tungjitkusolmun *et al.* [10] provide a detailed description of FEM modeling processes for RF ablation.

### A. The Bioheat Equation

The mechanism by which RF current induces tissue injury is the conversion of electric energy into heat. The circuit consists of the RF generator, the connecting wire to the distal electrodes, liver (and other tissues in the abdomen), a surface dispersive electrode, and the connecting wires to the generator that will complete the electric circuit. Joule heating arises when energy dissipated by an electric current flowing through a conductor is converted into thermal energy. The bioheat equation governs heating during hepatic ablation

$$\rho c \frac{\partial T}{\partial t} = \nabla \cdot k \nabla T + J \cdot E - h_{\mathrm{bl}}(T - T_{\mathrm{bl}}) - Q_{\mathrm{m}} \quad (1)$$

$$h_{\mathrm{bl}} = \rho_{\mathrm{bl}} c_{\mathrm{bl}} w_{\mathrm{bl}} \quad (2)$$

where $\rho$ is the density (kg/m$^3$), $c$ is the specific heat (J/kg · K), and $k$ is the thermal conductivity (W/m · K). $J$ is the current density (A/m$^2$) and $E$ is the electric field intensity (V/m) and can be calculated from the Laplace equation. $T_{\mathrm{bl}}$ is the temperature of the blood (assumed to be 37 °C), $\rho_{\mathrm{bl}}$ is the blood density (kg/m$^3$), $c_{\mathrm{bl}}$ is the specific heat of the blood (J/kg · K), and $w_{\mathrm{bl}}$ is the blood perfusion (1/s). $h_{\mathrm{bl}}$ is the convective heat transfer coefficient accounting for the blood perfusion in the model. The energy generated by the metabolic processes, $Q_{\mathrm{m}}$ (W/m$^3$), was neglected since it was small. The blood temperature in large vessels is unaffected by the thermal field in the surrounding tissue[13].

### B. Material Properties

We used the material properties required for solving the bioheat [(1)] from the literature [9], [14], [15]. Table I summarizes the material properties included in our FEM models. The blood perfusion in hepatic tissue, $w_{\mathrm{bl}}$, is $6.4 \times 10^{-3}$ 1/s [16].

### C. Software

We selected PATRAN version 7.0 (The MacNeal-Schwendler Co., Los Angeles, CA) to preprocess our FEM models. PATRAN allows users to create the geometric model, assign material properties to the appropriate regions, as well as specify the boundary conditions and loads. We can also mesh the models with PATRAN and then instruct it to generate an input file for the ABAQUS/Standard 5.8 (Hibbitt, Karlsson & Sorensen, Inc., Farmington Hills, MI) solver. ABAQUS is capable of solving the bioheat equation (1). We ran all numerical simulations on our HP-C180 workstation (with 1152 MB of RAM and about 34 GB of total disk space. For postprocessing, we employed the built-in module in ABAQUS, ABAQUS/POST, to generate temperature distribution profiles in each FEM analysis.

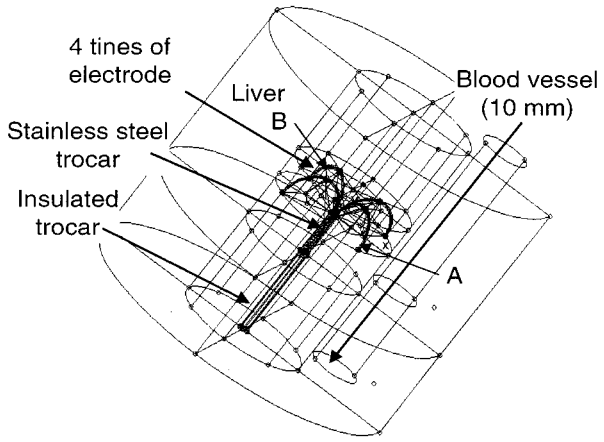


Fig. 2. FEM model for hepatic ablation using the RITA Medical System Model 30. The probe is fully deployed in the liver and a single 10-mm blood vessel is located 5 mm to the right of electrode A. This 3-D FEM model has 352 353 tetrahedral elements and 59 526 nodes.

### *D. Three-Dimensional FEM Analyses for Hepatic Ablation*

For all FEM analyses performed in this study, we used a RITA RF probe model 30. Fig. 2 shows the typical geometries of our FEM models. The RF probe was fully deployed (30-mm diameter) and was situated in the middle of the hepatic tissue. Although a temperature-sensing thermistor is embedded at the tip of each distal electrode in an actual probe, we excluded it from our models due to its small size. The 10-mm distal section of the stainless-steel trocar also conducts current while the remaining parts are insulated. To study the effect of the presence and the locations of a blood vessel, we performed 3-D FEM analyses for the following cases.

Case 1) No blood vessel was included in the model.

Case 2) A 10-mm-diameter blood vessel was 5 mm away from electrode A, parallel to the RF probe (shown in Fig. 2).

Case 3) A 10-mm-diameter blood vessel was 1 mm away from electrode A, parallel to the RF probe.

The overall FEM models had a cylindrical shape (100-mm diameter, 120-mm length), and contained approximately 350 000–370 000 tetrahedral elements and 59 500–65 000 nodes. We set the temperature on the boundary of the model to 37 °C. Using the Dirichlet boundary conditions, we assumed that the voltages on the outer surfaces of the model were 0 V. We simulated temperature-controlled ablations by varying the power applied to the electrodes. Temperature-controlled ablation was performed so that the maximum hepatic tissue temperatures were kept at 90 °C for 8 min in all cases. This setting is used in our university's hospital for clinical treatment. In the model the average applied power was 16 W, average voltage was 30 V, and impedance was 60 Ω. We define the lesion as the region having temperature above 50 °C at the end of the simulation.

### *E. 2-D Modeling With a Bifurcated Blood Vessel*

Since the actual vascular system in the liver is very complex, we also utilized a 2-D model to investigate the temperature distribution in hepatic tissue surrounded by a bifurcated blood vessel during RF ablation. The diameter of the bifurcated blood vessel varied from 5 to 10 mm. Fig. 3(a) and (b) shows different regions and the finite elements included in this model. The total number of triangular elements was 31 534. We constructed a 2-D model due to the limitation of our computing resource. The total number of tetrahedral elements required for a 3-D FEM model of a bifurcated blood vessel configuration is higher than in the previous section (straight cylindrical blood vessel). The 2-D model showed the complexity of the temperature profile within the hepatic tissue during RF ablation.

## III. Results

### *A. 3-D FEM Model of Hepatic RF Ablation in Homogeneous Hepatic Tissue (Case 1)*

Fig. 4(a) and (b) shows the cross-sectional temperature distribution and the extent of the lesion formation after 1 min, 90 °C RF ablation in homogeneous hepatic tissue. We can observe from Fig. 4(a) that the temperature distribution is symmetric between the two sides of the probe (electrodes A and B). The regions for the highest temperatures, or the "hot spots" were adjacent to electrodes A and B. Fig. 4(b) shows that the shape of the lesion generated by the RITA probe is mushroom-like. Certain regions between the fully deployed electrodes and the conducting trocar were not sufficiently heated to the lethal temperature (50 °C).

After 8 min, 90 °C RF ablation, the lesion extended further into the hepatic tissue by heat conduction and the temperature distribution was still symmetric [Fig. 4(c) and (d)]. The underdosed areas between electrodes A, B and the conducting trocar shown in Fig. 4(b) (1-min ablation) were sufficiently heated up to the lethal temperature after 8 min. Fig. 7 and Table II summarize the characteristics of the lesion. The diameter ($W_1 + W_2$) and the depth ($D_1 + D_2$) of the lesion were approximately 42 mm, and 36 mm, respectively. The lesion volume in this case was approximately 19.2 $cm^3$.

### *B. 3-D FEM Model With a 10-mm Diameter Blood Vessel Located at 5 mm From Electrode A (Case 2)*

Fig. 5 shows the temperature distribution of FEM analysis in case 2 after 8 min, 90 °C ablation. The characteristic of the lesion formed in this case was also mushroom-like, but it was slightly asymmetric due to the cooling effect of the blood vessel. Fig. 7 and Table II list the parameters associated with the lesion dimensions in this case. The location of the hot spot was adjacent to electrode A. This phenomenon was caused by the higher blood electrical conductivity, which diverted more RF current toward it. Thus, more Joule heating effect occurred in hepatic tissue between electrode A and the blood vessel. The diameter ($W_1 + W_2$) and the depth ($D_1 + D_2$) of the lesion were approximately 39 mm, and 34.1 mm, respectively. The lesion volume (18.6 $cm^3$) was slightly smaller than the lesion volume in case 1.

### *C. 3-D FEM Model With a 10-mm Diameter Blood Vessel Located 1 mm From Electrode A (Case 3)*

Fig. 6 shows the resulting temperature distribution in case 3. Unlike the results in the previous cases, the hot spot occurred next to electrode B, on the opposite side from the blood vessel. The characteristics of the lesion formation also resembled a mushroom shape, but the extent of the lesion was limited by

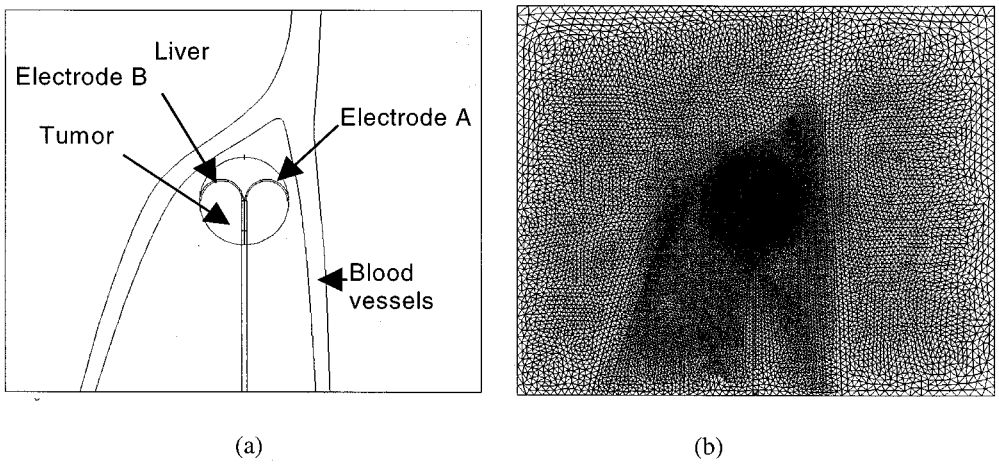


Fig. 3. (a) The 2-D FEM model with a bifurcated blood vessel. (b) The corresponding FEM mesh. This FEM model contains 31 534 elements and 15 918 nodes.

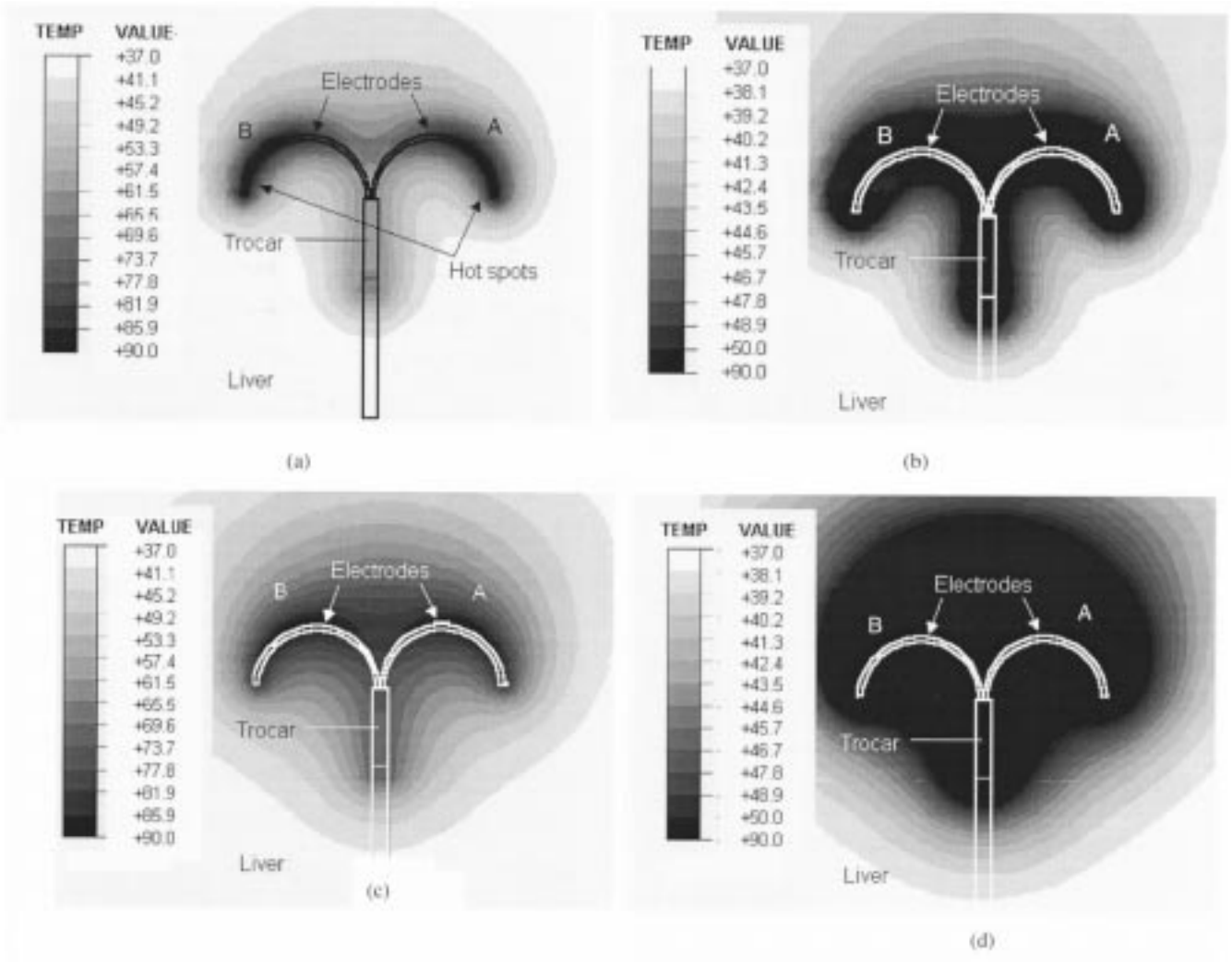


Fig. 4. (a). The cross-sectional temperature distribution for the FEM analysis in case 1, after 1 min of RF ablation. (b). The lesion formation (dark region in the center, temperature $\geq$50°C), after 1 min. (c). The temperature distribution after 8 min. (d). The lesion formation after 8 min. The viewing plane is (−1,1,0) (see Fig. 2 for the coordinates).

the blood vessel. Although there was more joule heating close to electrode A, the flowing blood in the vessel had a greater effect and dissipated thermal heat from the surrounding hepatic tissue. The diameter ($W_1 + W_2$) and the depth ($D_1 + D_2$) of the lesion were approximately 36 mm, and 33.3 mm, respectively. The lesion volume (17.2 $cm^3$) was 10.4% smaller than the lesion volume in case 1. Fig. 7 and Table II summarize the characteristics of the lesion formed in case 3.

TABLE II
THE RESULTING LESION DIMENSIONS OF DIFFERENT CASES. $V$ IS THE LESION VOLUME

| Case | $W_1$(mm) | $W_2$(mm) | $D_1$ (mm) | $D_2$ (mm) | $R_1$ (mm) | $R_2$ (mm) | $V$ (cm$^3$) |
|---|---|---|---|---|---|---|---|
| 1 | 21.0 | 21.0 | 17.6 | 18.5 | 11.8 | 11.8 | 19.2 |
| 2 | 18.9 | 20.0 | 17.9 | 16.2 | 10.9 | 10.7 | 18.6 |
| 3 | 15.8 | 20.0 | 17.5 | 15.8 | 12.8 | 10.4 | 17.2 |

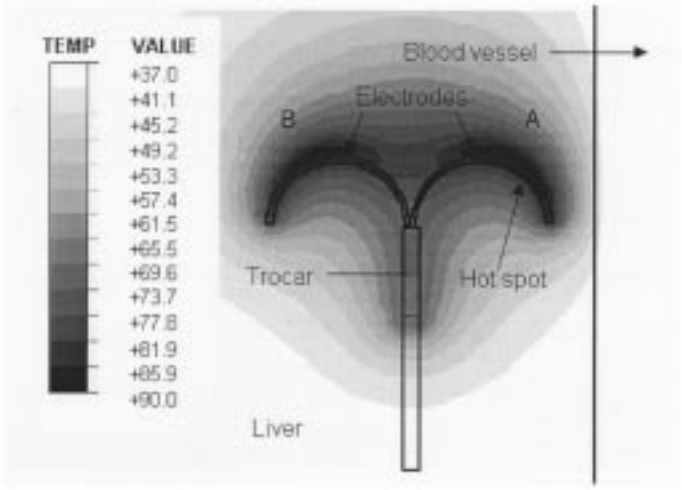


Fig. 5. The temperature distribution from the 3-D FEM model in a case where a 10-mm blood vessel is 5 mm from electrode A (case 2). The location of the maximum temperature ("hot spot") is adjacent to electrode A.

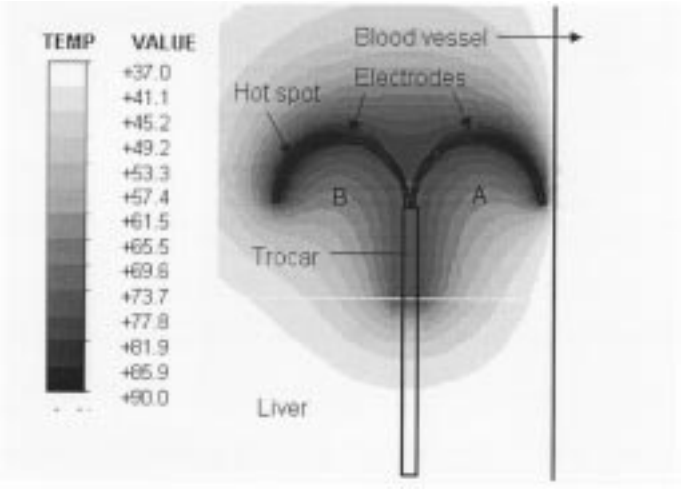


Fig. 6. The temperature distribution from the 3-D FEM model in a case where a 10-mm blood vessel is 1 mm from electrode A (case 3). The location of the hot spot is adjacent to electrode B.

### *D. 2-D FEM Model for Hepatic Ablation With a Bifurcated Blood Vessel*

Fig. 8 shows the temperature distribution of the 2-D bifurcated blood vessel after 8 min, 90 °C, RF ablation. The temperature distribution in this model was highly nonuniform. The location of the hot spot was next to the tip of electrode A. As previously discussed, the location of the hot spot is highly dependent on the distance between electrode and vessel. Since the tip of electrode A is at a different distance from the vessel than the tip of electrode B, we only see the hot spot at one electrode. Since this is a 2-D model, the temperatures in areas underneath

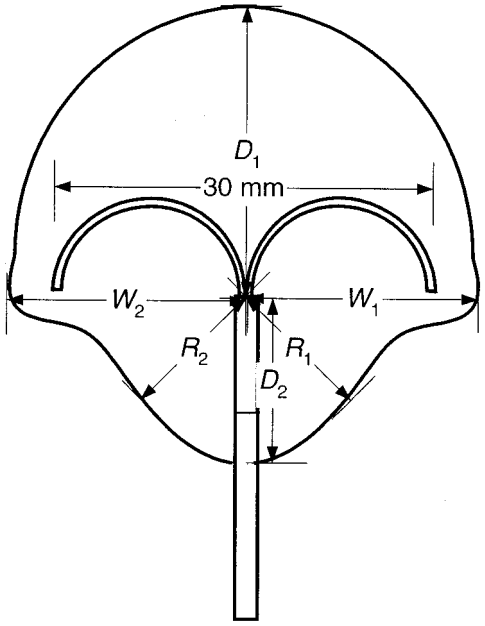


Fig. 7. The diagram of a typical lesion and the parameters measured.

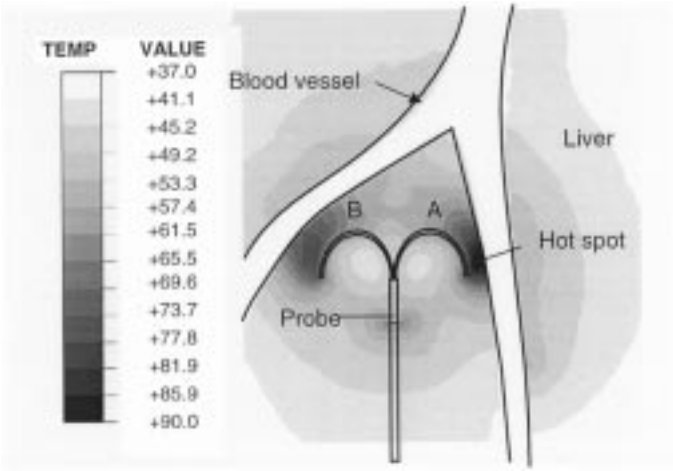


Fig. 8. The temperature distribution of the 2-D FEM model with a bifurcated blood vessel (shown in Fig. 3). High temperatures appear near the tip of electrode A.

the electrodes were likely underestimated. However, it is evident from the Fig. 8 that RF ablation under a complex vascular system has a potential to cause incomplete destruction of tumor cells.

## IV. CONCLUSION

We have illustrated, by employing FEM analyses, the characteristics of the lesions created by the conventional four-tine RF ablation probe. The lesion formed in homogeneous hepatic

tissue without blood vessels is predictable. However, the RF probe exhibits shortfalls in heating tissue surrounding the large blood vessel. The presence of large blood vessels in close proximity to the tumor has the following effects.

1) Since the blood has a higher electrical conductivity, it attracts RF current from the RF probe. This causes the temperature in hepatic tissue between the electrode and the blood vessel to rise due to the joule effect.
2) The flowing blood in the large vessel acts as a heat sink and dissipates thermal heat from the surrounding tissue.

The distance of the blood vessels from the tumor will determine the dominating factor and the location of the maximal tissue temperature. The results in Section IV show that when the distance of the blood vessel was 5 mm from the RF probe, factor one dominated. Thus, higher tissue temperature occurred near electrode A. In contrast, when the blood vessel was 1 mm away from the RF probe, the cooling effect dominated and cooled down the adjacent tissue. We also showed that the blood vessel bordered regions of lesion formation. Our results correlate with a previous study by Goldberg *et al.* [17].

Unlike our simplified FEM models, the liver is a very complex electrical and thermal organ due to its inhomogeneity. It is composed of three different types of blood vessels (hepatic arteries, portal veins, and hepatic veins) of different diameters and flow velocities, liver parenchyma, hepatic tumors, bile ducts, and stroma, all of which have unique electrical and thermal properties. We simplified the geometrical settings due to the limitation of our computing resource. With an increased computing capacity, we will be able to perform FEM analyses of more complex models. Future numerical studies will investigate different electrode designs for hepatic ablation. Some of the new probe designs that have recently been proposed are bipolar electrodes (current flowing between the electrodes), instead of monopolar (current flowing from the conducting electrodes to the dispersive electrode on the patient's body), or the cooled tip electrodes [18].

## REFERENCES


[1] S. A. Curley, F. Izzo, P. Delrio, L. M. Ellis, J. Granchi, P. Vallone, F. Fiore, S. Pignata, B. Banielle, and F. Cremona, "Radiofrequency ablation of unresectable primary and metastatic hepatic malignancies: Results in 123 patients," *Ann. Surg.*, vol. 230, pp. 1–8, 1999.

[2] J. P. McGahan, J. M. Brock, H. Tesluk, W.-Z. Gu, P. Schneider, and P. D. Browing, "Hepatic ablation with use of radio-frequency electrocautery in the animal model," *J. Vasc. Inter. Radiol.*, vol. 3, pp. 291–297, 1992.

[3] T. Livraghi, S. N. Goldberg, F. Monti, A. Bizzini, S. Lazzaroni, F. Meloni, S. Pellicano, L. Solbiati, and G. S. Gazelle, "Saline-enhanced radiofrequency tissue ablation in the treatment of liver metastases," *Radiology*, vol. 202, pp. 205–210, 1997.

[4] S. Rossi, E. Buscarini, R. Garbagnati, M. D. Stasi, P. Quaretti, M. Rago, A. Zangrandi, S. Andreola, D. Silverman, and L. Buscarini, "Percutaneous treatment of small hepatic tumors by an expandable RF needle electrode," *Amer. J. Radiol.*, vol. 170, pp. 1015–1022, 1998.

[5] S. Rossi, M. D. Stasi, E. Buscarini, P. Quaretti, F. Garbagnati, L. Squassante, C. T. Paties, D. E. Silverman, and L. Buscarini, "Percutaneous RF interstitial thermal ablation in the treatment of hepatic cancer," *Amer. J. Roentgenol.*, vol. 167, pp. 759–768, 1996.

[6] L. R. Jiao, P. D. Hansen, R. Havlik, R. R. Mitry, M. Pignatelli, and N. Habib, "Clinical short-term results of radiofrequency ablation in primary and secondary liver tumors," *Amer. J. Surg.*, vol. 177, pp. 303–306, 1999.

[7] S. H. Landis, T. Murray, S. Bolden, and P. A. Wingo, "Cancer statistics 1999," *CA: Cancer J. Clin.*, vol. 49, pp. 8–31, 1999.

[8] L. Solbiati, T. Ierace, S. N. Goldberg, S. Sironi, T. Livraghi, R. Fiocca, G. Servadio, G. Rizzatto, P. R. Mueller, A. D. Maschio, and G. S. Gazelle, "Percutaneous US-guided radiofrequency tissue ablation of liver metastases: treatment and follow-up in 16 patients," *Radiology*, vol. 202, pp. 195–203, 1997.

[9] D. Panescu, J. G. Whayne, S. D. Fleischman, M. S. Mirotznik, D. K. Swanson, and J. G. Webster, "Three-dimensional finite-element analysis of current density and temperature distributions during radio-frequency ablation," *IEEE Trans. Biomed. Eng.*, vol. 42, pp. 879–890, Sept. 1995.

[10] S. Tungjitkusolmun, E. J. Woo, H. Cao, J. Tsai, V. R. Vorperian, and J. G. Webster, "Thermal-electrical finite-element modeling for radio-frequency cardiac ablation: effects of changes in myocardial properties," *Med. Biol. Eng. Comput.*, vol. 38, pp. 562–568, 2000.

[11] S. Tungjitkusolmun, E. J. Woo, H. Cao, J.-Z. Tsai, V. R. Vorperian, and J. G. Webster, "Finite-element analyses of uniform current density electrodes for radio-frequency cardiac ablation," *IEEE Trans. Biomed. Eng.*, vol. 47, pp. 32–40, Jan. 2000.

[12] M. G. Curley and P. S. Hamilton, "Creation of large thermal lesions in liver using saline-enhanced RF ablation," in *Proc. 19th Annu. Int. Conf. IEEE Eng. Med. Biol. Soc.*, Chicago, IL, 1997, pp. 2516–2519.

[13] J. Chato, "Heat transfer to blood vessels," *ASME Trans. Biomech. Eng.*, vol. 102, pp. 110–118, 1980.

[14] J. W. Valvano, J. R. Cochran, and K. R. Diller, "Thermal conductivity and diffusivity of biomaterials measured with self-heating thermistors," *Int. J. Themophys.*, vol. 6, pp. 301–311, 1985.

[15] T. E. Cooper and G. J. Trezek, "A probe technique for determining the thermal conductivity of tissue," *J. Heat Transfer, Trans. ASME*, vol. 94, pp. 133–140, 1972.

[16] E. S. Ebbini, S.-I. Umemura, M. Ibbini, and C. A. Cain, "A cylindrical-section ultrasound phased-array applicator for hyperthermia cancer therapy," *IEEE Trans Sonics Ultrason.*, vol. SU-35, pp. 561–572, 1988.

[17] S. N. Goldberg, G. S. Gazelle, L. Solbiati, T. Livraghi, K. K. Tanabe, P. F. Hahn, and P. R. Mueller, "Ablation of liver tumors using percutaneous RF therapy," *Amer. J. Roentgenol.*, vol. 170, pp. 1023–1028, 1998.

[18] Y. Miao, Y. Ni, S. Mulier, K. Wang, M. Hoey, P. Mulier, F. Penninckx, J. Yu, I. D. Scheerder, A. L. Baert, and G. Marchal, "Ex vivo experiment on radiofrequency liver ablation with saline infusion through a screw-tip cannulated electrode," *J. Surg. Res.*, vol. 71, pp. 19–24, 1997.

[19] M. W. Miller and M. C. Ziskin, "Biological consequences of hyperthermia," *Ultrasound Med. Biol.*, vol. 15, pp. 707–722, 1989.

[20] S. A. Sapareto and W. C. Dewey, "Thermal dose determination in cancer therapy," *Int. J. Radiation Oncol. Biol. Phys.*, vol. 10, pp. 787–800, 1984.

[21] J. P. McGahan and G. D. Dodd, "Radiofrequency ablation of the liver: current status," *Amer. J. Radiol.*, vol. 176, pp. 3–16, 2001.


**Supan Tungjitkusolmun** (S'96–M'00) was born in Bangkok, Thailand, December 5, 1972. He received the B.S.E.E. degree from the University of Pennsylvania, Philadelphia, in 1995, and the M.S.E.E. and Ph.D. degrees from the University of Wisconsin, Madison, in 1996, and 2000.

He is on the faculty of the Department of Electronics, Faculty of Engineering, and the Research Center for Communications and Information Technology, King Mongkut's Institute of Technology Ladkrabang, Bangkok, Thailand. His research interests include finite-element modeling, radio-frequency cardiac ablation, and hepatic ablation.

He is a member of Tau Beta Pi, Eta Kappa Nu, and Pi Mu Epsilon.

**S. Tyler Staelin** attended the University of Michigan, Ann Arbor, and Vanderbilt University School of Medicine, Nashville, TN, prior to training in surgery at the University of Wisconsin Hospital and Clinics, Madison.

He Chief Resident in Surgery at the University of Wisconsin Hospital and Clinics

**Dieter Haemmerich** (S'00) was born in Vienna, Austria on May 22, 1971. He received the B.S.E.E. degree from the Technical University of Vienna, Austria in 1997 and the M.S.B.M.E. degree from the University of Wisconsin, Madison, in 2000. He is currently working toward the Ph.D. degree in the Department of Biomedical Engineering, University of Wisconsin.

His research interests include finite-element analysis of radio frequency ablation and tissue impedance measurement.

**Jang-Zern Tsai** (S'97) was born in Chia-Yi, Taiwan, in 1961. He received the B.S.E.E. degree from National Central University, Chung-Li, Taiwan, in 1984, and the M.S.E.E. degree from National Tsing Hua University, Hsinchu, Taiwan, in 1986. In 2001, he received the Ph.D. degree in electrical and computer engineering from the University of Wisconsin, Madison, doing research on myocardial resistivity measurement.

He joined the Industrial Technology Research Institute (ITRI) as an Integrated Circuit Applications Engineer and as a Hardware Engineer on digital recording technology. In 1990, he joined the Computer and Communication Research Laboratories of ITRI as a Hardware Engineer on digital recording technology and the Accton Technology Corporation as a Software Engineer. He is presently a Postdoctoral Fellow at the University of California developing hardware for electrical impedence tomography

**Hong Cao** (S'97) received the B.S. and M.S. degrees in electrical engineering from Nanjing University, Nanjing, China in 1992 and 1995, respectively. He received the Ph.D. degree in electrical and computer engineering at the University of Wisconsin, Madison, in 2001.

Currently, he is a Senior Software Developer at Epic System Corporation, working on enterprise electronic medical record (EMR) database system and integration of medical instruments into EMR system. His research interests include medical instrumentation, RF catheter ablation of cardiac tissue and hepatic tumor, and medical information system.

He is contributing author to J. G. Webster (Ed.), *Minimally Invasive Medical Technology* (Bristol, U.K.: IOP Publishing, 2001).

**John G. Webster** (M'59–SM'69–F'86–LF'97) received the B.E.E. degree from Cornell University, Ithaca, NY, in 1953, and the M.S.E.E. and Ph.D. degrees from the University of Rochester, Rochester, NY, in 1965 and 1967, respectively.

He is Professor of Biomedical Engineering at the University of Wisconsin-Madison. In the field of medical instrumentation, he teaches undergraduate and graduate courses, and does research on radio–frequency cardiac and hepatic ablation.

Dr. Webster is editor of *Medical instrumentation: application and design, 3rd edition* (New York: Wiley, 1998), *Encyclopedia of electrical and electronics engineering* (New York: Wiley, 1999), and *Minimally invasive medical technology* (Bristol, U.K.: IOP Publishing, 2001). He is the recipient of the 2001 EMBS Career Achievement Award.

**Fred T. Lee Jr.** received the BA and M.D. degrees from Boston University, Boston, MA, in 1984 and 1986, respectively.

After serving a residency in diagnostic radiology at The University of Rochester, Rochester, N.Y., he became a Faculty Member at the University of Wisconsin, Madison. He has been the Director of Abdominal Radiology since 2000. His research interests are in tumor ablation and radiographic contrast materials for the detection of cancer.

**David M. Mahvi** received the B.S. degree in microbiology and premed from the University of Oklahoma, Norman, in 1977 and the M.D degree from the University of South Carolina, Columbia, in 1981. He then competed the following postgraduate medical clinical training programs at Duke University, Durham, NC: residency in surgery from 1981–1983; fellowship in immunology 1983–1985; residency in surgery 1985–1989.

In 1989, he joined the Section of Surgical Oncology, Department of Surgery at the University of Wisconsin-Madison where he is Professor of Surgery. He is Staff Surgeon, Oncologic and General Surgery, Middleton Memorial Veterans Hospital, Madison, WI and Member, University of Wisconsin Comprehensive Cancer Center.

**Vicken R. Vorperian** received the M.D. degree in 1985 from the American University of Beirut, Beirut, Lebanon. He did a fellowship in cardiac arrhythmias and electrophysiology at the Vanderbilt University, Nashville, TN; and fellowship in cardiac pacing and catheter ablation at the University of Michigan, Ann Arbor, MI.

He is Clinical Associate Professor of Medicine in the Department of Medicine, University of Wisconsin-Madison and is an electrophysiologist in the Cardiac Electrophysiology Laboratory at the University of Wisconsin Hospital. He is also a member of the Arrhythmia Consultants of Milwaukee S.C., a private practice group in cardiac arrhythmias and clinical cardiac electrophysiology.